ELSEVIER

Available online at www.sciencedirect.com

SCIENCE DIRECT®

Chemical Physics Letters 375 (2003) 177–184

CHEMICAL PHYSICS LETTERS

www.elsevier.com/locate/cplett

# Silicon carbide hollow nanospheres, nanowires and coaxial nanowires

Guozhen Shen, Di Chen, Kaibin Tang *, Yitai Qian, Shuyuan Zhang

*Department of Chemistry and Structure Research Laboratory, University of Science and Technology of China, Hefei 230026, People's Republic of China*

Received 28 February 2003; in final form 9 May 2003

## Abstract

The synthesis and characterization of hollow nanospheres, nanowires and coaxial nanowires of cubic phase silicon carbide (β-SiC) were reported. The reaction between $SiCl_4$ (or Si powders), $C_6Cl_6$ and sodium was used to prepare SiC nanostructures at different temperature. The samples were characterized by X-ray powder diffraction (XRD), transmission electron microscopy (TEM), electron diffraction (ED), high-resolution transmission electron microscopy (HRTEM), Raman, photoluminescence (PL) and X-ray photoelectron spectroscopy (XPS) procedures. Studies found that temperature and reagents were key factors for the samples' morphologies.

## 1. Introduction

In recent years, one of the important goals of material Scientists is to develop ways of tailoring the structure of materials on specific nanomorphologies [1]. The shape and size of inorganic nanomaterials are well known to have an important influence on their widely varying electrical and optical properties [2], which is important in various application, such as catalysis [3], solar cells [4], light-emitting diodes [5], and biological labeling [6]. In the specific nanomorphologies, the hollow sphere structures which have potential for encapsulation of large quantities of guest molecules or large-sized guests within the empty core domain, are being attracted considerable attention because of their specific structure and potential applications. And one-dimensional nanorods, which can be used as building blocks for many novel functional materials, are also of great interests to materials scientists.

Since cubic silicon carbide (β-SiC) possesses unique physical and electronic properties [7], it is therefore a suitable material for the fabrication of electronic devices operating at high-temperature, high power, and high frequency, and in harsh environment [8]. The conventional process for the preparation of SiC powders is the carbonthermal reduction of silica [9], the self-propagating high-temperature synthesis (SHS) [10], polysilane polymer precursors [11], sol–gel [12], plasma [13], and microwave radiation [14] technologies

---

* Corresponding author. Fax: +86-551-3601-600.
*E-mail address:* gzsh@mail.ustc.edu.cn (K. Tang).

0009-2614/03/$ - see front matter © 2003 Published by Elsevier Science B.V.
doi:10.1016/S0009-2614(03)00877-7

and so on. Recently, many other convenient methods have also been used to prepare SiC crystals [15–21].

In the present study, SiC hollow nanospheres and nanowires were synthesized at 600 and 700 °C, respectively, by using $SiCl_4$ and $C_6Cl_6$ as source materials, and metallic sodium as the reductant. And the coaxial SiC/C nanowires were synthesized at 700 °C by the reaction between Si, $C_6Cl_6$ and sodium. Studies revealed that temperature and reagents were key factors for the morphologies of the products. To the best of our knowledge, there is no report on the synthesis of SiC hollow nanosphere structure.

## 2. Experimental

### 2.1. General procedures

All of the manipulations were carried out in a dry glove box filled with flowing argon. All reagents were analytically pure and purchased from Shanghai Chemistry and used without further purification. Before use, the Si powders were grounded.

### 2.2. Preparation of SiC hollow nanospheres

In a typical experimental procedure, appropriate amounts of $SiCl_4$ (3.0 ml), $C_6Cl_6$ (1.2 g), and Na (3.5 g) were put into a stainless steel autoclave of 30-ml capacity. After being sealed, the autoclave was maintained in a furnace at 600 °C for 5–12 h and then cooled to room temperature in the furnace naturally. The product was collected and washed with absolute alcohol. And then treated by $H_2SO_4$ and HF to remove amorphous silicon and other impurities, then washed with distilled water to eliminate NaCl and other impurities. After being dried in vacuum at 70 °C for 3 h, a gray-white sample was obtained.

### 2.3. Preparation of SiC nanowires

The reaction was conducted analogously to that above, but the autoclave with the same amounts of reactants was maintained at 700 °C for 5–12 h. The product was treated as above. After being dried in vacuum, a gray-white sample was obtained.

### 2.4. Preparation of coaxial SiC/C nanowires

In a typical procedure, appropriate amounts of Si powders (0.6 g), $C_6Cl_6$ (1.0 g) and metal Na (1.5 g) were put into an autoclave. After being sealed, the autoclave was maintained at 650–700 °C for 10 h and then cooled to room temperature naturally. The product was collected and treated also as the above. After dried in vacuum, a gray-white product was obtained.

### 2.5. Characterization

X-ray powder diffraction (XRD) patterns were carried out on a Rigaku D/max $\gamma$A X-ray diffractometer equipped with a graphite monochromatized Cu K$\alpha$ radiation ($\lambda = 1.541$ Å). The samples were scanned at a scanning rate of 0.05°/s in the $2\theta$ range of 20–80°.

Transmission electron microscopy (TEM) images were taken with a Hitachi H-800 transmission electron microscope, using an accelerating voltage of 200 kV.

The high-resolution transmission electron microscopy (HRTEM) images and energy dispersive spectrum (EDS) pattern were taken on a JEOL-2010 transmission electron microscope with an attached EDS system.

X-ray photoelectron spectroscopy (XPS) was recorded on a VGESCALAB MKII X-ray photoelectron spectrometer, using nonmonochromatized Mg K$\alpha$ X-ray as the excitation source.

The Raman spectra were produced at room temperature with a LABRAM-HR Confocal Laser MicroRaman spectrometer. Photoluminescence (PL) spectra of the samples were measured in a Hitachi 850 fluorescence spectrophotometer with a Xe lamp at room temperature.

## 3. Results and discussion

Phase identification of as-prepared samples was carried out using the XRD patterns. Fig. 1 shows

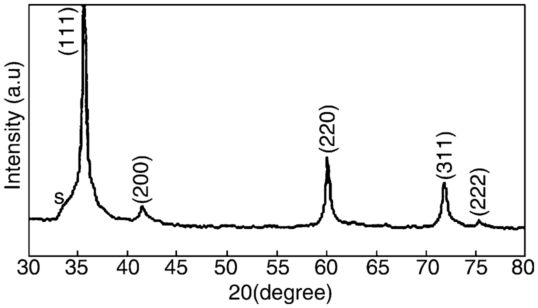

Fig. 1. XRD pattern of SiC synthesized at 600 °C. ('s': stacking faults).

the typical XRD pattern of the sample prepared at 600 °C by the reaction between $SiCl_4$, $C_6Cl_6$ and sodium. All of the strong intensity peaks could be indexed to the β-SiC structure with a low-intensity peak at $d = 2.675$ Å which may be due to stacking faults [22] (marked with s). The refinement gave the cell constant, $a = 4.3606$ Å, which was consistent with the reported value in the literature ($a = 4.3589$ Å, JCPDS card, No. 29-1129). No peaks of other impurities, such as Si, $SiO_2$, could be detected in the pattern.

Fig. 2 shows the TEM images and electron diffraction (ED) pattern of the samples. Fig. 2a is the image of SiC hollow nanospheres prepared at 600 °C. It can be seen that typical SiC hollow nanospheres are 50–100 nm in diameters and 10 nm in the shell thickness. The corresponding ED pattern is shown in Fig. 2b. The three polycrystalline rings in accordance with β-SiC [(1 1 1), (2 2 0) and (3 1 1)] confirm the XRD result. Besides the hollow nanospheres, some nanowires and nanoparticles are also observed. The yield of SiC hollow nanospheres to the total product is about 75%.

The morphology of SiC nanowires synthesized at 700 °C is shown in Figs. 2c,d. It can be seen that the sample consists mainly of nanowires. The SiC nanowires produced from present route typically have diameters of 20 nm and lengths up to 10 μm.

Figs. 2e,f show the TEM images of the samples prepared from Si, $C_6Cl_6$ and sodium at 700 °C. Fig. 2e reveals the general view of morphology of SiC nanowires. Further insight into the structure

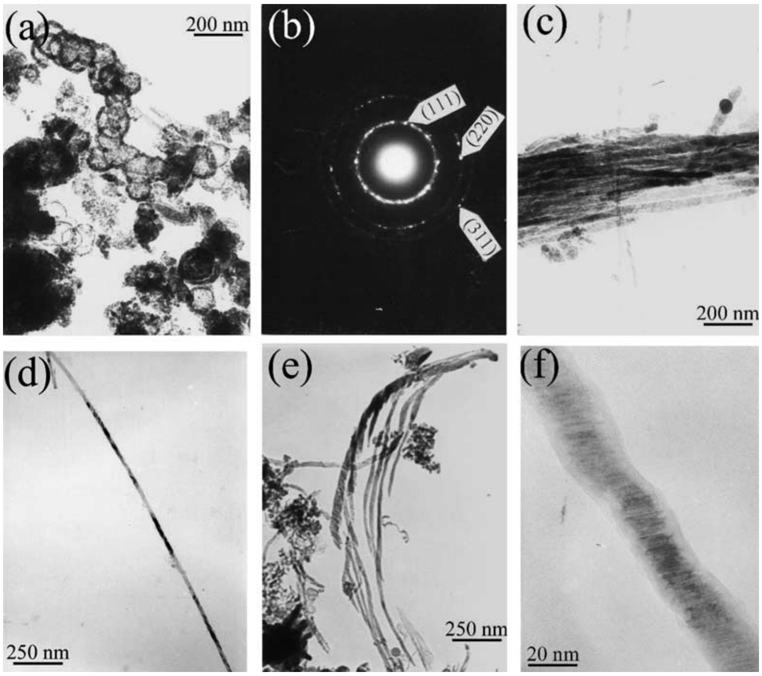

Fig. 2. (a) TEM image of SiC hollow nanospheres. (b) ED pattern of SiC hollow nanospheres. (c) TEM image of SiC nanowires. (d) TEM image of a single SiC nanowire. (e) TEM image of coaxial SiC/C nanowires. (f) TEM image of a single coaxial SiC/C nanowire.

of the nanowires shows that each individual nanowire is actually a hierarchical nanowires, in which a center thinner nanowire is wrapped in a uniform outer layer. The result is shown in Fig. 2f. It can be seen that the center thinner nanowires are about 20 nm in diameter and several micrometers in length. The outer layer is with a thickness of about 4 nm.

ED and HRTEM are performed in order to obtain information about the structure of the SiC nanostructures. The results are shown in Fig. 3. The HRTEM image of SiC hollow nanospheres is shown in Fig. 3a, which suggests that the SiC hollow nanospheres are composed of well-crystallized little SiC nanoparticles. The lattice fringes are 0.25 nm corresponding to (1 1 1) of SiC. ED pattern inset shows its polycrystalline nature, it also confirms the XRD pattern. The inner zone of SiC hollow nanosphere is marked with arrow on the image.

Fig. 3b demonstrates that the transparent section of the SiC nanowires is well-defined 3*C*-SiC single crystal. The lattice fringes along the orientation of the nanorod are 0.25 nm, indicating that the nanowires have grown in a $\langle 1\,1\,1 \rangle$ direction. The ED pattern inset is the corresponding pattern recorded along the [1 1 0] zone axis. There are some stacking faults in this SiC nanorod. The stacking fault planes are parallel to the $\{1\,1\,1\}$ crystal planes and the angle between the two groups of stacking fault plane is 70.5°.

Fig. 3c is the representative lattice-resolved image of a coaxial SiC/C nanowire. The spacing of the crystallographic planes measured from the HRTEM image is 0.25 nm. It corresponds to the $\{1\,1\,1\}$ lattice planes of the crystalline SiC, which indicates that the center thinner nanowires is β-SiC. The HRTEM analysis also reveals that the outer layer of the coaxial nanowire is amorphous phase. EDS analysis of the outer layer shows the presence of carbon and absence of Si, which reveals that the outer layer is composed of amorphous carbon instead of amorphous SiO$_2$. The result is in consistent with [20]. There is a high density of stacking faults and a few twins (so-called microtwins) on the image. The inset ED pattern is recorded along the [1 1 0] zone axis.

X-ray photoelectron spectra (XPS) are measured to derive composition information about the samples. Fig. 4a depicts high-resolution XPS

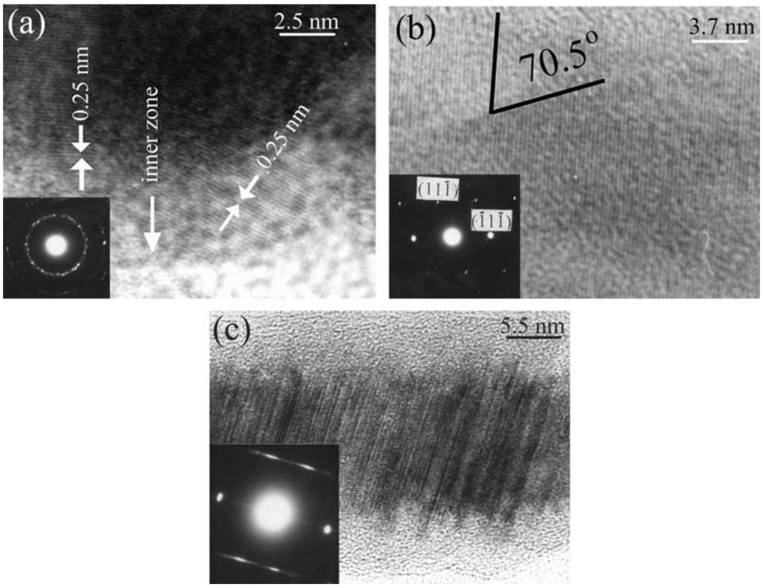

Fig. 3. (a) HRTEM image of SiC hollow nanospheres. (b) HRTEM image of SiC nanowires. (c) HRTEM image of coaxial SiC/C nanowires.

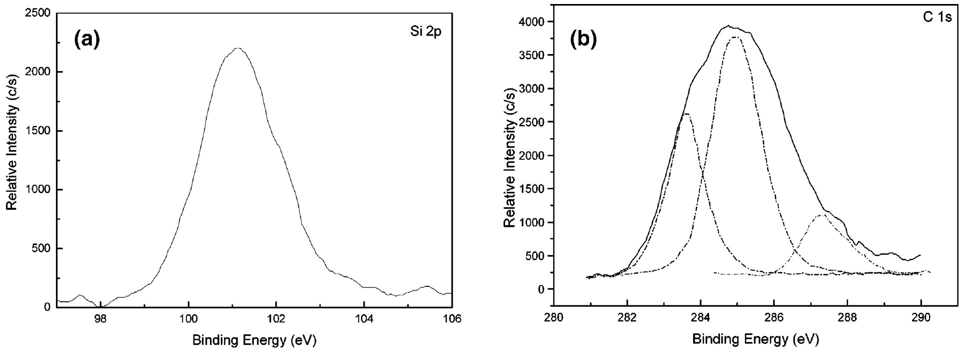

Fig. 4. XPS spectrum of coaxial SiC/C nanowires.

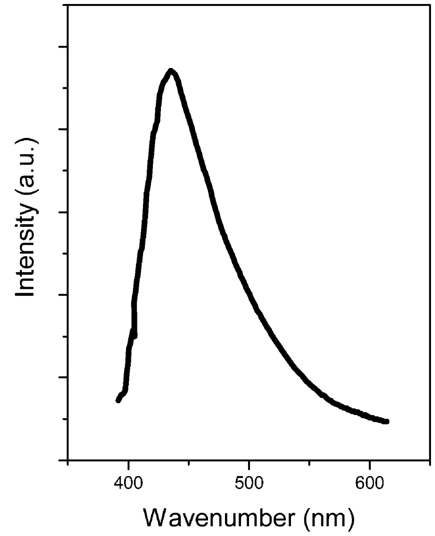

Fig. 5. Photoluminescence spectra for the SiC hollow nanospheres at room temperature.

spectrum taken for the Si regions of the coaxial SiC/C nanowires. It displays a peak at 101.05 eV corresponding to the Si 2p binding energy of SiC. No obvious peak of Si 2p binding energy of $SiO_2$ could be detected. Fig. 4b is the C regions of the sample. It displays three peaks. The peak at 283.1 eV corresponds to C 1s binding energy of SiC. The other peaks can be attributed to the carbon (284.3 eV for C 1s in graphite) of the outer carbon layer and the adsorbed $CO_2$ at the powders' surface. All the analyses (EDS and XPS) indicate that the outer layer of the coaxial nanowires is carbon instead of amorphous $SiO_2$.

The as-obtained SiC nanostructures were also characterized by Raman procedure (figures were not shown here). The Raman spectrum of as-prepared SiC nanowires shows the presence of a sharp peak at 780 $cm^{-1}$, which confirms that the nanorods are well crystalline β-SiC [23].

The PL spectra from the SiC hollow nanospheres at room temperature were shown in Fig. 5. The excitation wavelength was 385 nm and the filter wavelength was 430 nm. It was clear that a strong peak centered at 435 nm is observed. The results were in good agreement with the reported value [24].

In present studies, it was found that temperature was important on the formation of SiC nanostructures. In our experiments of preparation of SiC hollow nanospheres and nanowires, we found that if the temperature was lower than 550 °C, no SiC crystallites could be detected on the XRD pattern. Temperature higher than 550 °C resulted in the appearance of SiC crystallite. But the sample was composed of a large amount of amorphous product. If the reaction temperature was 600 °C, XRD pattern showed the peaks of only SiC crystalline. High-resolution electron microscopy image revealed that this sample was hollow nanospheres consisted of high crystallized SiC nanoparticles. But when the temperature was as high as 700 °C, almost pure SiC nanowires would be obtained instead of SiC hollow nanospheres. Temperature between 600 and 700 °C resulted in the co-existence of SiC hollow nanospheres and nanowires. If the temperature was higher than 750 °C, the diameters of SiC nanowires increased easily. So the suitable temperature we selected was 600 °C for SiC hollow nanospheres and 700 °C for SiC nanowires. For the preparation of the coaxial SiC/C nanowires, temperature lower than 600 °C resulted in no desired sample but amorphous product. The optimum reaction condition for the coaxial SiC/C nanowires was at the temperature of 700 °C for 10 h. The whole results are shown in Table 1.

In our synthetic route, selecting $C_6Cl_6$ as reactant is a key factor to the formation of SiC hollow nanospheres and SiC/C coaxial nanowires, when other carbon source, such as $CCl_4$, activated carbon substituted $C_6Cl_6$, only SiC nanowires or nanoparticles could be obtained.

From Table 1, one can see that the selected reactants also result in different reaction temperature to the formation of cubic phase SiC. For example, crystalline SiC can be obtained by co-reduction of $CCl_4$ and $SiCl_4$ at 400 °C, the reaction temperature will be raised to 600 °C by substitution of $C_6Cl_6$ for $CCl_4$, these results could be attributed to the different molecular configuration of $CCl_4$ and $C_6Cl_6$. C (Si) atom in $CCl_4$ ($SiCl_4$) molecule is $sp^3$ hybridization which is consistent with the C (Si) atom configuration in SiC crystal, crystalline SiC would be obtained at relatively low temperature by reaction of $SiCl_4$ and $CCl_4$. Unlike $CCl_4$, C atoms in $C_6Cl_6$ molecule are $sp^2$ hybridization and a quite stable conjugated $\pi$ system is formed, it is expected that extra energy is needed to activate carbons in $C_6Cl_6$. Therefore, the reaction temperature of $C_6Cl_6$ and $SiCl_4$ will be raised in order to obtain crystalline SiC. Similar results occur by substitution of Si for $SiCl_4$.

In our present work, crystalline SiC can be obtained based on the following reactions:

$$6SiCl_4 + C_6Cl_6 + 30Na \rightarrow 6SiC + 30NaCl \qquad (1)$$

$$6Si + C_6Cl_6 + 6Na \rightarrow 6SiC + 6NaCl \qquad (2)$$

In previous work, we found that if $C_6Cl_6$ was reduced by sodium at 600 °C, the product we got was amorphous carbon hollow nanospheres with diameters of 50–120 nm, carbon hollow nanospheres were observed even though the reduction temperature was as high as 700 °C. The TEM images show that the SiC hollow nanospheres prepared by co-reduction of $SiCl_4$ and $C_6Cl_6$ at 600 °C have diameters of 50–100 nm, which almost hold the shape and the diameter size of carbon hollow nanospheres skeleton. So it is reasonable to expect that carbon hollow nanospheres may be the reaction intermediate and may act as an in situ template in the formation of SiC hollow nanospheres [16,25,26].

On the basis of the above analyses, the formation mechanism of SiC nanostructures could be proposed although the exact formation mechanism is not completely understood. From the formation enthalpies of $SiCl_4$ ($H_f = -627.71$ kJ/mol) and $C_6Cl_6$ ($H_f = -127.6$ kJ/mol), it is desirable for $C_6Cl_6$ to be reduced by sodium firstly through deleting chloro to form planar carbon clusters at relatively low temperature and then carbon clusters will form metastable sphere aggregate, subsequently, $SiCl_4$ will be reduced to form activate Si particles. Once the reaction is initiated, the heat generated in the process is sufficient to melt the byproduct NaCl (bp = 801 °C) and vaporize the reductant Na (bp = 889 °C); the newly formed Si particles will be dispersed in the NaCl molten flux. On the other hand, most of the carbon intermediates may be still hold sphere aggregates under such a condition and they are also dispersed in the

Table 1
Relationship between the sample morphologies and reagents temperature

| Reagents | Temperature (°C) | Morphology |
|---|---|---|
| $SiCl_4 + C_6Cl_6 + Na$ | 600 | Hollow nanospheres |
| | 600–700 | Hollow nanospheres and nanowires |
| | 700 | Nanowires with very little amounts of hollow nanospheres |
| $Si + C_6Cl_6 + Na$ | 700 | Coaxial SiC/C nanowires |
| $SiCl_4 + C + Na$ [19] | 600 | Nanocrystallines |
| $Si + CCl_4 + Na$ [20] | 700 | Nanowires |
| $SiCl_4 + CCl_4 + Na$ [21] | 400 | Nanowires |

NaCl molten flux. The molten NaCl would be an interface of solid–solid or solid–gas reaction and may serve as a medium for the crystallization of SiC. Thus, the newly formed Si and gaseous $SiCl_4$ would surround the carbon sphere aggregates and react with them to form SiC polycrystalline hollow nanospheres. The schematic formation process of SiC hollow nanospheres could be formulated as followed:

$$n\mathrm{C_6Cl_6} + 6n\mathrm{Na} \rightarrow 6n\mathrm{C}\ (\text{cluster}) + 6n\mathrm{NaCl} \rightarrow \mathrm{C}\ (\text{sphere aggregate}) \tag{3}$$

$$\mathrm{SiCl_4} + 4\mathrm{Na} \rightarrow \mathrm{Si} + 4\mathrm{NaCl} \tag{4}$$

$$\mathrm{Si} + \mathrm{C} \rightarrow \mathrm{SiC} \tag{5}$$

$$\mathrm{SiCl_4} + 4\mathrm{Na} + \mathrm{C} \rightarrow \mathrm{SiC} + 4\mathrm{NaCl} \tag{6}$$

When the reaction temperature is raised to 700 °C, in the early time, the procedure is similar to that at 600 °C. Once the reaction is initiated, the energy produced in reaction is so large that it may be sufficient to break the C–C bonds in $C_6Cl_6$ molecules due to the higher reaction temperature. In this case, the newly formed Si particles in the molten NaCl may act as the energetically favored site and directly react with gas-phase reactants $C_6Cl_6$ (bp = 325 °C) and Na. Thus a vapor–liquid–solid (VLS) process is established to the growth of the SiC nanowires. Such a process is similar to the route of [21]. In our experiment, liquid globules were found on the tip of the nanowires on the TEM image, which suggested the VLS mechanism was dominant in the SiC nanowires growth. Therefore, the products prepared by co-reduction of $SiCl_4$ and $C_6Cl_6$ at 700 °C are mainly SiC nanowires with a small amount of SiC hollow nanospheres.

As for the reaction of Si and $C_6Cl_6$, the initial reaction temperature is 700 °C. The thermodynamics parameter calculation shows that the reaction is thermodynamically spontaneous ($\Delta G_f^0 = -2682.5$ kJ/mol) and highly exothermic ($\Delta H_f^0 = -2731.4$ kJ/mol), suggesting that a large amount of heat also generated in the process, which is sufficient to activate Si and break C–C bond in the $C_6Cl_6$ molecule. Thus a VLS process is also employed to the growth of SiC nanowires, which is similar to the route of [20]. Noting that the enthalpy of the reaction is much lower than that of reaction (1) and the whole heat capacities of the products ($C_p = 631.5$ kJ/mol) are higher than that of the reactants ($C_p = 499.06$ kJ/mol). It is expected that, along with the proceeding of the reaction, the heat generated in the reaction would be insufficient to break C–C bond in the $C_6Cl_6$ molecules. Therefore, in the later stage of the reaction, the amorphous carbon reduced by Na would be created and deposited on the surface of SiC nanowires to form an amorphous sheath, thus coaxial SiC/C nanowires could be obtained.

The feature of the present route is an initially high pressure in the autoclave, which comes from the vaporization of $C_6Cl_6$ (bp = 325 °C) and/or $SiCl_4$. It facilitates the nucleation of SiC nanostructures, similar to [20], and makes the crystalline SiC form at relatively low temperature.

## 4. Conclusion

In conclusion, we succeeded in synthesizing β-SiC hollow nanospheres, nanowires and coaxial nanowires via a simple reaction at mild conditions. Studies showed that the temperature and reagents were key factors of the formation of SiC nanostructures. Given the generality of this method, it can be in principle used to synthesize other carbides, such as TiC, ZrC and VC, etc. The intensive studies are in progress.

## Acknowledgements

This work is supported by Chinese National Science Research Foundation and the 973 Projects of China.

## References

[1] S. Iijima, Nature 354 (1991) 56.
[2] C.M. Lieber, Solid State Commun. 107 (1998) 607.
[3] T.S. Ahmadi, Z.L. Wang, T.C. Green, A. Henglein, M.A. Elsayed, Science 272 (1996) 1294.
[4] W. Hynh, X. Peng, A.P. Alivisatos, Adv. Mater. 11 (1999) 923.

[5] M.C. Schlamp, X.G. Peng, A.P. Alivisatos, J. Appl. Phys. 82 (1997) 5837.

[6] W.C.W. Chan, S.M. Nie, Science 281 (1998) 2016.

[7] R.F. Davis, J.W. Palmour, J.A. Edmond, Diamond Relat. Mater. 1 (1992) 109.

[8] P.M. Ajayan, T.W. Ebbesen, T. Ichihashi, S. Iijima, K. Tanigak, H. Hiura, Nature (Lond.) 362 (1993) 522.

[9] J.J. Biernacki, G.P. Wotzak, J. Am. Ceram. Soc. 72 (1989) 122.

[10] J. Narayan, R. Raghunathan, R. Chowdhury, K. Jagannadham, J. Appl. Phys. 75 (1994) 7252.

[11] A.A. Maher, K. Bruce King, M.K. Abraham, Eur. Polym. J. 28 (1992) 315.

[12] I.S. Seog, C.H. Kim, J. Mater. Sci. 28 (1993) 3227.

[13] J.Y. Guo, F. Gitzhofer, M.I. Boulos, J. Mater. Sci. 30 (1995) 5589.

[14] P.D. Ramesh, B. Vaidhyanathan, M. Ganguli, R.J. Rao, J. Mater. Res. 9 (1994) 3025.

[15] J.J. Ritter, US Patent 4 606 902, August 19, 1986.

[16] H.J. Dai, E. Wong, Y.Z. Lu, S.S. Fan, C.M. Lieber, Nature (Lond.) 375 (1995) 769.

[17] W.Q. Han, S.S. Fan, Q.Q. Li, B.L. Gu, D.P. Yu, Chem. Phys. Lett. 265 (1997) 374.

[18] G.W. Meng, L.D. Zhang, C.M. Mo, S.Y. Zhang, Y. Qin, S.P. Feng, H.J. Li, J. Mater. Res. 13 (1998) 2533.

[19] J.Q. Hu, Q.Y. Lu, K.B. Tang, Y.T. Qian, G.E. Zhou, X.M. Liu, J.X. Wu, Chem. Mater. 11 (1999) 2369.

[20] J.Q. Hu, Q.Y. Lu, K.B. Tang, B. Deng, R.R. Jiang, Y.T. Qian, W.C. Yu, G.E. Zhou, X.M. Liu, J.X. Wu, J. Phys. Chem. B 104 (2000) 5251.

[21] Q.Y. Lu, J.Q. Hu, K.B. Tang, Y.T. Qian, G.E. Zhou, X.M. Liu, J.S. Zhu, Appl. Phys. Lett. 75 (1999) 507.

[22] Y.G. Gogotsi, K.G. Nickel, D.B. Hourlier, T.M. Mejean, G.E. Khouienko, K.P. Skjerlie, J. Mater. Chem. 6 (1996) 595.

[23] P.V. Huong, Mater. Sci. Eng. B 11 (1992) 235.

[24] W.Q. Han, S.S. Fan, Q.Q. Li, W.J. Liang, B.L. Gu, D.P. Yu, Chem. Phys. Lett. 265 (1997) 374.

[25] W.Q. Han, S.S. Fan, Q.Q. Li, Y. Hu, Science 227 (1997) 1287.

[26] W.Q. Han, S.S. Fan, Q.Q. Li, B.L. Gu, X.B. Zhang, D.P. Yu, Appl. Phys. Lett. 71 (1997) 2271.